Journal of Molecular Graphics and Modelling 29 (2011) 935–946

Contents lists available at ScienceDirect

Journal of Molecular Graphics and Modelling

journal homepage: www.elsevier.com/locate/JMGM

Iso-energetic multiple conformations of hypermodified nucleic acid base wybutine (yW) which occur at 37th position in anticodon loop of tRNA^{Phe}

Navanath M. Kumbhar [b], Kailas D. Sonawane [a,*]

[a] Structural Bioinformatics Unit, Department of Biochemistry, Shivaji University, Kolhapur 416 004, Maharashtra (M.S.), India
[b] Department of Biotechnology, Shivaji University, Kolhapur 416 004, Maharashtra (M.S.), India

ARTICLE INFO

Article history:
Received 25 December 2010
Received in revised form 27 March 2011
Accepted 29 March 2011
Available online 12 April 2011

Keywords:
Wybutine (yW)
Hypermodified nucleoside
Molecular dynamics (MD) simulations
PCILO
DFT

ABSTRACT

Conformational preferences of wybutine (yW) have been studied by quantum chemical semi-empirical Perturbative Configuration Interaction with Localized Orbitals (PCILO) and PM3 methods. Automated full geometry optimization by using RM1 along with *ab-initio* Hartree–Fock (HF-SCF) and Density Functional Theory (B3LYP/6-31G**) calculations have also been made to compare the salient features. Molecular dynamics (MD) simulation has been performed to see the solvation effect on wybutine side chain. The preferred conformations of wybutine side chain spreads away 'distal' from five membered imidazole moiety of tricyclic base. The intramolecular interactions provide stability to the preferred wybutine structure. The most stable and alternative stable structures obtained by PCILO and PM3 methods reveal that wybutine side chain may have multiple iso-energetic conformations. Molecular dynamics (MD) simulation study also confirms multiple conformations of wybutine side chain by showing regular periodical fluctuations over the 2 ns time period. These fluctuations occur when torsion angle α takes value $\pm 90^{\circ}$ and $\pm 120^{\circ}$ as observed in the most stable and alternative stable structures resulted by PCILO and PM3 methods. Such conformational behavior of wybutine may have certain implications on frameshifting to prevent extended Watson–Crick base pairing by maintaining proper codon–anticodon interactions during protein biosynthesis process.

© 2011 Elsevier Inc. All rights reserved.

1. Introduction

Hypermodified nucleosides naturally occur in the anticodon loop of diverse tRNAs specific to various amino acids [1–3]. These modified nucleosides occur at the 'Wobble' (34th) and at the 3′-adjacent (37th) position in anticodon loop of tRNA [4–6]. Modifications present at the 37th position may help define the proper reading frame for codon–anticodon interactions whereas modifications occur at the wobble position extend or restrict the selection of synonymous codons to be read by the tRNA [7]. Modifications present at 34th and 37th positions may also optimize the strength of codon–anticodon interactions to enable smooth and in phase protein biosynthesis process [8,9]. The nature of the chemical modification of the nucleic acid base present at 3′-adjacent (37th) position to the anticodon correlates with the nature of the third base of the anticodon [2,3,10–14]. In tRNAs with the anticodon terminating in adenosine (A), the hydrophobic modified base, N6-Δ^2-isopentenyladenosine (i^{6}A) or it's derivative 2-methylthio-N6-Δ^2-isopentenyladenosine (ms^{2}i^{6}A), occur at 3′-adjacent to the anticodon loop [5,13,14]. In contrast to this tRNA molecules with anticodon ending in Uridine (U), the 3′-adjacent hypermodified nucleic acid base is hydrophilic substituted N6-threonylcarbonyl adenosine, t^{6}Ade, or it's 2-methylthio derivative, ms^{2}tc^{6}Ade, or it's 2-methyl derivative, m^{6}tc^{6}Ade, or N6-glycylcarbonyl adenosine, gc^{6}Ade [6,13,14].

Wybutosine (yW) is one of the most extensively hypermodified and highly fluorescent nucleoside, which naturally occur at the 3′-adjacent position in the anticodon loop of eukaryotic phenylalanine tRNA [15–17]. The structure of the fluorescent yW base was deduced by ultraviolet (UV), nuclear magnetic resonance (NMR), and mass spectroscopic methods [18]. Wybutosine maintains proper reading frame by stabilizing codon–anticodon interactions during decoding process on the ribosomes [19]. It has been shown that tRNA^{Phe} that lacks wybutosine modification enhance frameshifting, which results in replication of human immunodeficiency virus (HIV) RNA [20,21]. Effect of wybutine base modification on frame shifting is small but at least measurable [22]. Disruption of the yW base modification from anticodon loop of tRNA^{Phe} may result in some pathological consequences, produce local changes in anticodon conformation and may also have long range perturbations on tRNA^{Phe} tertiary structure [23,24]. Removal

* Corresponding author. Tel.: +91 988 1320719/231 2609153; fax: +91 231 2692333.
E-mail address: kds_biochem@unishivaji.ac.in (K.D. Sonawane).

1093-3263/$ – see front matter © 2011 Elsevier Inc. All rights reserved.
doi:10.1016/j.jmgm.2011.03.005

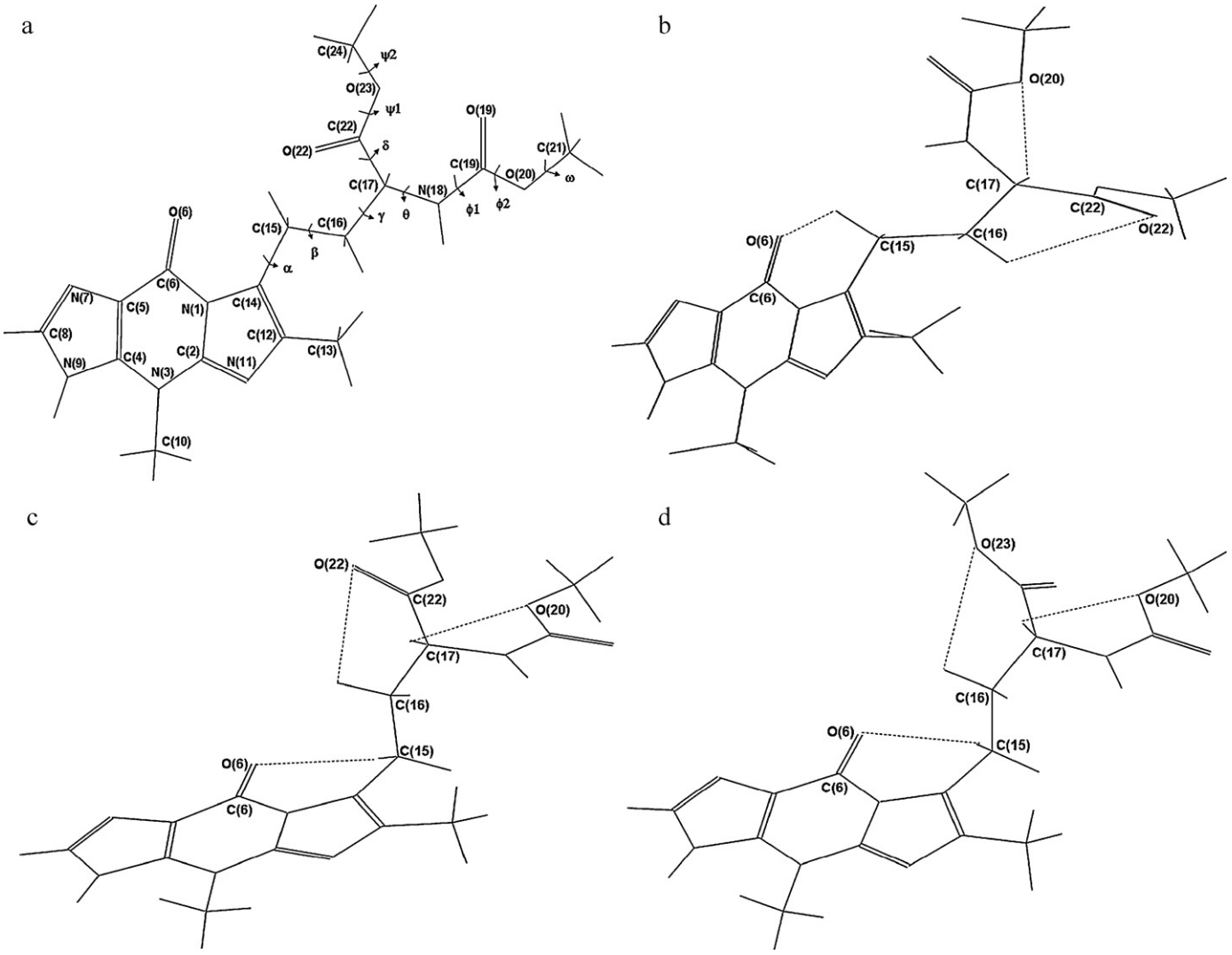

Fig. 1. (a) Starting geometry of yW for PM3 and PCILO conformational energy calculations. (b) PM3 predicted most stable structure. (c) 1st slightly higher energy alternative stable structure. (d) 2nd slightly higher energy alternative stable structure.

of yW base from anticodon loop of $tRNA^{Phe}$ causes a partial unwinding of the anticodon stem and consequently decreases in the high temperature stability of the tRNA molecule [25].

Conformational behavior of wybutine (yW) has been the focus of discussion since long time. Temperature jump measurements using fluorescence Y37 base as a probe have shown that $tRNA^{Phe}$ may exists in two conformations in solution [26]. Similarly, other studies have also reported that wybutine exists in two different conformations [27,28]. Nonetheless, three possible states i.e. low, intermediate and high rotational mobilities of Y37 base have also been investigated in another fluorescence study [29]. Ground state and excited state properties of wybutine were studied by using configuration interaction singles (CIS) and time dependent density functional (TDDFT) methods [30]. It has been demonstrated by using semi-empirical quantum chemical AM1 calculations that some noticeable conformational change occurs in the wybutine side chain at 37th position when first uracil of codon UUC binds to the A36 of anticodon GAA of $tRNA^{Phe}$ [31]. It has also been concluded that the hypermodified Y base may provide electrostatic interactions for the energetic of codon–anticodon pairing [32] which may consequently help in gene expression. Molecular dynamics simulation study of yeast $tRNA^{Phe}$ anticodon domain in the presence and absence of codon trinucleotides UUC and UUU also show that there are small but identifiable differences found near the Y37 base [33]. The wybutine may have certain fluctuations with codon binding.

However, all the above discussed studies give information about the conformational behavior of hypermodified nucleoside wybutosine either as a part of anticodon loop of $tRNA^{Phe}$ or in the bound form with anticodons and codons. Till now we do not have clear information about the different conformations of wybutine side chain at atomic level. The conformational preferences of isolated wybutine base have not been studied earlier. Hence, in accordance with experimental results [26–29], present theoretical study have been undertaken to understand the multiple conformational behavior of wybutine side chain. Conformational study of wybutine by quantum chemical semi-empirical PCILO and PM3 methods along with molecular dynamics (MD) simulation results show that wybutine side chain prefers multiple iso-energetic conformations.

2. Nomenclature, conventions and approach

Fig. 1a illustrates the atom numbering and identification of various torsion angles, which determines the relative orientation of various atoms in hypermodified nucleic acid base wybutine (yW). The torsion angle α [C(12)–C(14)–C(15)–C(16)] is measured with respect to C(12) from the eclipsed (0°) position between the terminal bonds C(12)–C(14) and C(15)–C(16) in the right hand sense of

Table 1
Geometrical parameters for hydrogen bonding interactions from preferred conformation of wybutine (yW) obtained by PM3 and PCILO calculations along with crystal structure conformer (1EHZ).

Methods	Atoms involved (1–2–3)	Distance atom pair 1–2 (A°)	Distance atom pair 2–3 (A°)	Angle 1–2–3 (degree)	Figure Ref.
PM3	O(6)···HC(15)	2.428	1.073	110.93	1b, 1c, 1d
	O(20)···HC(17)	2.581	1.073	94.61	1b, 1c, 1d
	O(22)···HC(16)	2.713	1.073	98.32	1b, 1c
	O(23)···HC(16)	2.750	1.073	98.77	1b, 1c
	O(22)···HC(16)	2.709	1.073	98.51	1d
	O(23)···HC(16)	2.753	1.073	98.57	1d
PCILO	O(6)···HC(16)	2.181	1.073	117.24	2a, 2b, 2c
	O(6)···HN(18)	1.767	1.014	157.11	2a, 2b, 2c
	O(22)···HC(15)	2.452	1.073	93.52	2a, 2c
	O(6)···HC(16)	2.169	1.073	118.05	2d
	O(22)···HC(15)	2.661	1.073	131.09	2d
	O(20)···HC(24)	2.893	1.073	106.32	2c
	O(23)···HC(15)	2.410	1.073	93.71	2b
	O(23)···HC(16)	2.702	1.073	93.81	2d
Crystal conformer 1EHZ.pdb [35]	O(6)···HC(15)	2.342	1.073	115.95	2e
	O(6)···HN(18)	2.326	1.014	165.91	2e
	O(20)···HC(17)	2.861	1.073	90.45	2e
	O(22)···HC(16)	2.518	1.073	97.44	2e
	O(20)···HC(24)	2.680	1.073	162.75	2e

rotation around the central bond C(14)–C(15). Likewise the successive bonds along with the main extension of the substituent define the subsequent torsion angles β [C(14)–C(15)–C(16)–C(17)], γ [C(15)–C(16)–C(17)–N(18)], δ [C(16)–C(17)–C(22)–O(23)], $\psi 1$ [C(17)–C(22)–O(23)–C(24)], $\psi 2$ [C(22)–O(23)–C(24)–H], θ [C(16)–C(17)–N(18)–C(19)], $\varphi 1$ [C(17)–N(18)–C(19)–O(20)], $\varphi 2$ [N(18)–C(19)–O(20)–C(21)], ω [C(19)–O(20)–C(21)–H] are measured. For conformation with $\alpha = 180^\circ$ the bond C(15)–C(16) points towards the five membered imidazole moiety of guanine and is termed as 'proximal'. In case of $\alpha = 0^\circ$ the bond C(15)–C(16) points away from the cyclic five membered imidazole moiety of guanine and the conformation is termed as 'distal'. Fig. 1a depicts all trans (extended, 180°) conformation with exception of α torsion angle (conformation is 'distal'), which is positioned as eclipsed by taking torsion angle value as $\alpha = 0^\circ$. The reference source data [34] appropriate for the bonding environment of the hydrogen atoms and the data from the crystal structure observations on similar systems [35,36] are utilized for the nonhydrogenic atoms.

3. Computational methods

3.1. Conformational search

Conformational energy calculations have been carried out with the help of quantum chemical Perturbative Configuration Interaction with Localized Orbitals (PCILO) method [37–39]. Throughout the conformational search polarity of the chemical bonds has been optimized for every molecular conformation. Energy correction terms up to the third order are included in the calculations of total ground state energy. This method has been found widely useful in conformational studies of variety of bioorganic molecules [40], including nucleic acid constituents and its derivatives [41]. Variation of total energy with respect to torsion angles determining the base substituent orientation in the modified wybutine (yW) has been investigated. In the multidimensional conformational space logical selection of grid points approach is used for searching the most stable structure and the alternative stable structure [42]. Variations of the total ground state energy with the torsion angles are defining the base substituent orientation has been studied by changing torsion angles. One torsion angle is changed at a time over the entire range of 0–360°, at 30° intervals. Favored values of each torsion angle yielding energy minima are thus determined. By using these favored values various possible combinations for the set of dihedral angles are then tried out, and the combination yielding the overall minimum energy is selected. Starting with the conformation so arrived, each torsion angle is again individually varied over the entire range (0–360°) as already described. In this way, fine adjustments in the torsion angles lowering energy still further can be revealed. From these freshly arrived torsion angles new combinations of dihedral angles for stable molecular conformations may be derived as in the previous step. In this manner, the stability of the arrived conformation, with respect to changes in any of the various torsion angles, besides its preeminence is also ensured. In all PCILO calculations bond lengths and bond angles in the wybutine side chain retain similar values. For rotation around all the exocyclic chemical bonds rigid body internal rotation has been assumed. Earlier conformational preferences of various modified nucleic acid bases and protonation induced conformational changes of these have been studied by PCILO method [43–49].

To check the conformational behavior of wybutine (yW) side chain we have also performed another conformational search by semi-empirical PM3 method. Single point energy calculations have been made by PM3 method to search the energetically preferred conformation of wybutine (yW). All the energy calculation steps and procedures followed in PM3 are same as discussed above in PCILO method. For conformational energy calculations the starting geometry of hypermodified nucleic acid base wybutine (yW) has been kept same for both the PCILO and PM3 methods. The PM3 method is implemented in commercially available *PC Spartan Pro* (version 6.1.1.0, Wavefunction Inc.) software [50].

3.2. Automated geometry optimization

Relative stability of salient points has been examined using automated complete geometry optimization calculation using semi-empirical quantum chemical RM1 [51] methods. Relative preferences of salient features have also been deduced using *ab-initio* molecular orbital Hartree–Fock (HF-SCF) quantum mechanical energy calculations by using 6-31G** basis set and Density Functional Theory (DFT) by using B3LYP 6-31G** [52,53] basis

Table 2
Torsion angle values for alternative stable conformations of wybutine (yW) obtained by PM3 and PCILO calculations and for crystal structure conformer of yW (1EHZ).

Torsion angles (degree)	Rel. energy (kcal/mol.)	Figure Ref.
$\alpha = 90^\circ$, $\beta = 180^\circ$, $\gamma = 300^\circ$, $\delta = 90^\circ$, $\psi 1 = 180^\circ$, $\psi 2 = 180^\circ$, $\theta = 150^\circ$, $\varphi 1 = 0^\circ$, $\varphi 2 = 180^\circ$, $\omega = 180^\circ$	0.0	1b
$\alpha = 270^\circ$, $\beta = 180^\circ$, $\gamma = 300^\circ$, $\delta = 90^\circ$, $\psi 1 = 180^\circ$, $\psi 2 = 180^\circ$, $\theta = 150^\circ$, $\varphi 1 = 0^\circ$, $\varphi 2 = 180^\circ$, $\omega = 180^\circ$	0.36	1c
$\alpha = 270^\circ$, $\beta = 180^\circ$, $\gamma = 300^\circ$, $\delta = 270^\circ$, $\psi 1 = 180^\circ$, $\psi 2 = 180^\circ$, $\theta = 150^\circ$, $\varphi 1 = 0^\circ$, $\varphi 2 = 180^\circ$, $\omega = 180^\circ$	0.40	1d
$\alpha = 90^\circ$, $\beta = 180^\circ$, $\gamma = 300^\circ$, $\delta = 90^\circ$, $\psi 1 = 180^\circ$, $\psi 2 = 180^\circ$, $\theta = 150^\circ$, $\varphi 1 = 180^\circ$, $\varphi 2 = 180^\circ$, $\omega = 180^\circ$	0.59	–
$\alpha = 120^\circ$, $\beta = 150^\circ$, $\gamma = 300^\circ$, $\delta = 120^\circ$, $\psi 1 = 180^\circ$, $\psi 2 = 180^\circ$, $\theta = 150^\circ$, $\varphi 1 = 180^\circ$, $\varphi 2 = 180^\circ$, $\omega = 180^\circ$	0.0	2a
$\alpha = 120^\circ$, $\beta = 150^\circ$, $\gamma = 300^\circ$, $\delta = 300^\circ$, $\psi 1 = 180^\circ$, $\psi 2 = 180^\circ$, $\theta = 150^\circ$, $\varphi 1 = 180^\circ$, $\varphi 2 = 180^\circ$, $\omega = 180^\circ$	0.13	2b
$\alpha = 120^\circ$, $\beta = 150^\circ$, $\gamma = 300^\circ$, $\delta = 120^\circ$, $\psi 1 = 180^\circ$, $\psi 2 = 180^\circ$, $\theta = 150^\circ$, $\varphi 1 = 0^\circ$, $\varphi 2 = 180^\circ$, $\omega = 180^\circ$	0.25	2c
$\alpha = 240^\circ$, $\beta = 150^\circ$, $\gamma = 180^\circ$, $\delta = 300^\circ$, $\psi 1 = 180^\circ$, $\psi 2 = 180^\circ$, $\theta = 150^\circ$, $\varphi 1 = 180^\circ$, $\varphi 2 = 180^\circ$, $\omega = 180^\circ$	2.6	2d
$\alpha = 80^\circ$, $\beta = 142^\circ$, $\gamma = 300^\circ$, $\delta = 251^\circ$, $\psi 1 = 296^\circ$, $\psi 2 = 180^\circ$, $\theta = 188^\circ$, $\varphi 1 = 355^\circ$, $\varphi 2 = 300^\circ$, $\omega = 180^\circ$	–	2e

set. These methods (RM1, HF-SCF and DFT) are implemented in commercially available *PC Spartan Pro* (version 6.1.1.0, Wavefunction Inc.) software [50].

3.3. Molecular dynamics simulation protocol

Molecular dynamics (MD) simulation were performed using Sybyl 7.3 [54] commercial software from Tripos, Inc. in order to highlight the influence of water solvation on wybutine molecule. The predicted preferred conformation of wybutine obtained from PM3 conformational analysis was used as a starting geometry for molecular dynamic simulations. The calculations were performed on HP xw8600 workstation. Kollman-all-atom force field [55] with Gasteiger–Marsilli charges and TIP3P model water has been chosen for molecular dynamics (MD) simulation study. Minimal cubic periodic boundary condition of diameter 35.968 Å has been applied. Trajectories are taken for time span of 10 ps. The constant temperature (canonical ensemble) simulation at 300 K has been used along with 8 Å-non bonded cut off and dielectric function 'constant' held at 1. For temperature ramp from 0 K to 200 K, 10 ps interval of 50 K and for 200 K to 300 K, 10 ps interval of 25 K temperature steps are used. The other usual conditions applied include 1 fs time step, initial Boltzmann velocity distribution, and shake algorithm for hydrogen atoms, 10 fs non-bonded update with scaled velocities. To remove steric clashes initially, 5000 cycles of steepest descent minimization steps are applied to the whole system. This minimized system considered for 200 ps equilibration protocol followed by 5000 cycles of steepest descent energy minimization. Final system is subjected for 2 ns of production run time by maintaining all the parameters as described earlier.

4. Results and discussion

4.1. Conformational preferences of wybutine (yW) by semi-empirical PM3 method

The predicted most stable conformation of wybutine (yW) by using quantum chemical semi-empirical PM3 is shown in Fig. 1b. The torsion angles describing the preferred conformation are ($\alpha = 90^\circ$, $\beta = 180^\circ$, $\gamma = 300^\circ$, $\delta = 90^\circ$, $\psi 1 = 180^\circ$, $\psi 2 = 180^\circ$, $\pm 300^\circ$, $\theta = 150^\circ$, $\varphi 1 = 0^\circ$, $\varphi 2 = 180^\circ$, $\omega = 180^\circ$, $\pm 300^\circ$). Preferred orientation of wybutine side chain is such that methyoxycarbonyl–aminocarboxypropyl group spreads away 'distal' from the five membered imidazole moiety of modified tricyclic guanine base. The O(6) of modified tricyclic base involved in hydrogen bonding (Table 1) with HC(15) along with O(20)···HC(17) is responsible for maintaining the 'distal' conformation of wybutine side chain. Preferred conformation (Fig. 1b) is stabilized by intramolecular hydrogen bonding (Table 1) between O(6)···HC(15) and O(20)···HC(17). Additional stabilization is also expected from intramolecular interactions between O(22)···HC(16) and O(23)···HC(16). The orientation of carboxy methyl (–COOCH3) group of wybutine side chain i.e. C(22)–O(22)–O(23)–CH3 prefers towards the –CH3 group of five membered tricyclic ring. This kind of orientation is possible may be because of rotation of torsion angles $\gamma = 300^\circ$ and $\delta = 90^\circ$ which results in interaction of HC(16) with that of O(22) and O(23). Hence, the carboxy methyl (–COOCH3) group of wybutine side chain may have certain interactions with codons if present at 3′-end and such interactions are also discussed by Neto and co-workers [31,32].

Flipping of torsion angle α to 270° results in higher energy (0.36 kcal/mol) alternative stable conformation (Fig. 1c) shown in Table 2. This alternative conformation is stabilized by intramolecular interactions between O(6)···HC(15), whereas atom HC(16) forms a hydrogen bonding O(22) and O(23) of wybutine side chain. This alternative conformation of wybutine (Fig. 1c) differs only in torsion angle 'α' while all other torsion angle values remain same. In this alternative conformation the amino carboxyl group (NHCOOCH3) of wybutine side chain occupies position on the side of –CH3 group of five membered tricyclic ring in place of carboxyl methyl (COOCH3) as found in the most stable conformation (Fig. 1b). Hence, the atoms O(22) and O(23) may not be available to participate in bonding with codons if present at 3′ side as shown in earlier study [31,32]. Another slightly higher energy (0.4 kcal/mol) alternative conformation (Fig. 1d) arises by flipping of torsion angle α to 270° and δ to 270° as shown in Table 2. The intramolecular interaction between O(6)···HC(15) remain as a stabilizing factor whereas other interactions O(23)···HC(16) and O(20)···HC(17) may also contribute in providing stability for this alternative conformation (Fig. 1d). Another (0.59 kcal/mol) alter-

Table 3
Optimized torsion angle values for wybutine (yW) after performing automated complete geometry optimization through RM1, HF-SCF and DFT methods.

Methods	Torsion angles (degree)										Starting structure
	α	β	γ	δ	$\psi 1$	$\psi 2$	θ	$\varphi 1$	$\varphi 2$	ω	
RM1	101	176	293	77	179	181	175	355	184	180	Fig. 1b
HF-SCF	104	169	295	101	181	181	174	352	181	180	
DFT	105	164	297	104	181	181	171	354	181	180	
RM1	101	173	287	72	177	181	182	185	180	180	Fig. 2a
HF-SCF	102	163	291	80	180	181	188	181	180	180	
DFT	104	161	293	90	181	181	183	179	179	178	
RM1	101	176	294	290	181	180	177	352	181	181	Fig. 2e
HF-SCF	103	169	295	274	341	185	176	349	179	181	
DFT	104	164	296	266	346	184	176	352	179	184	

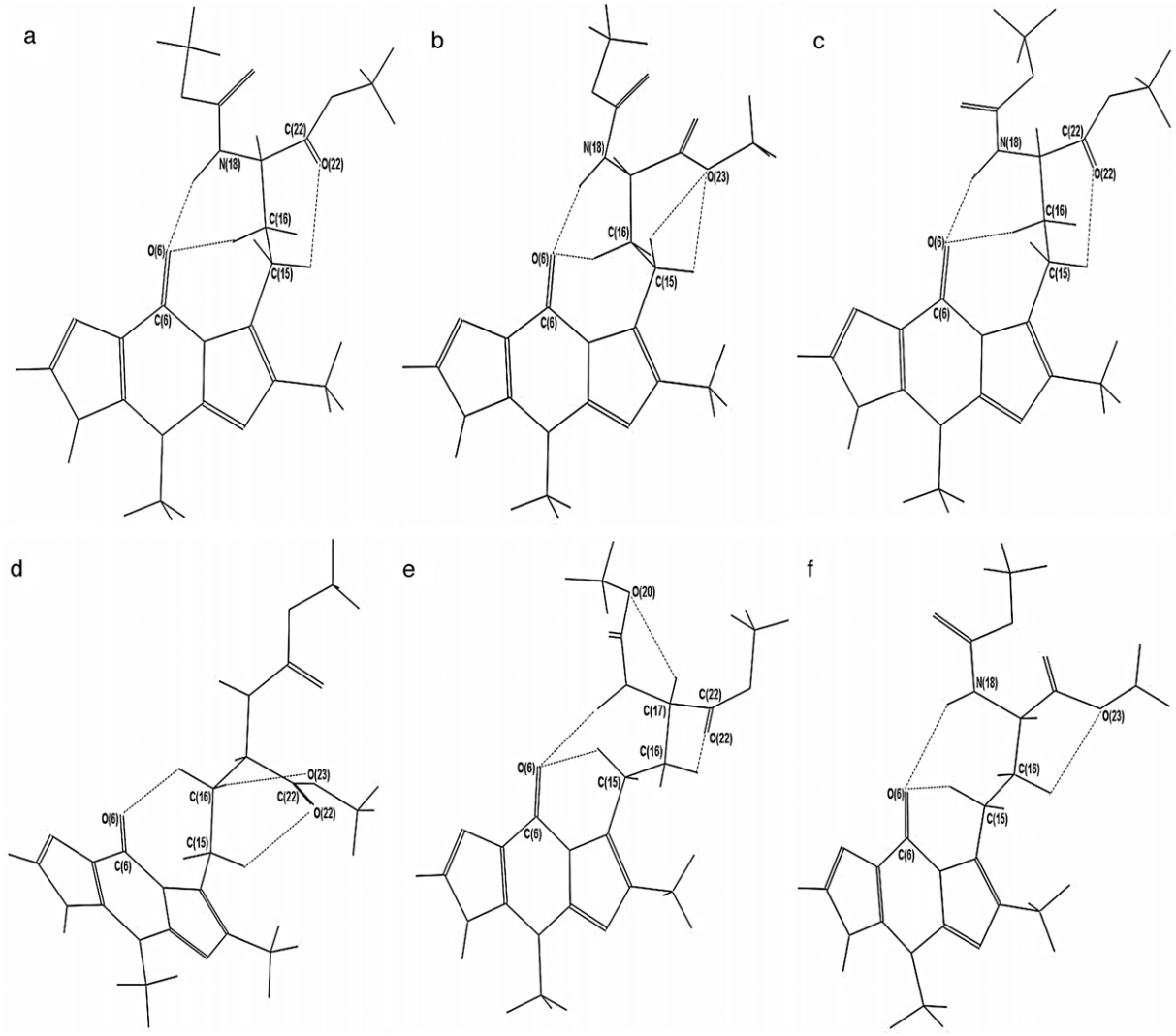

Fig. 2. (a) PCILO predicted most stable structure of wybutine. (b) 1st slightly higher energy stable alternative structure. (c) 2nd higher energy stable alternative structure. (d) 3rd higher energy stable alternative conformation. (e) Isolated wybutine side chain extracted from crystal structure (1EHZ.pdb)[35]. (f) RM1 optimized structure of wybutine side chain separated from (1EHZ.pdb).

native conformation expected when torsion angle $\varphi 1$ takes 180° as compared to PM3 most stable structure (Fig. 1b).

These three alternative conformations discussed above do not differ energetically to large extent as compared to the predicted most stable structure (Fig. 1b). The torsion angle α may prefer ±90° value according to the most stable structure (Fig. 1b) and alternative stable structures (Fig. 1c and d) of wybutine side chain. These conformations (Fig. 1b–d) might interchange pretty much easily during codon–anticodon interactions as relative energy differences are very less. Such conformational changes have also been described in earlier experimental studies [26–29]. Thus, the PM3 most stable structure (Fig. 1b) and alternative stable structures (Fig. 1c and d) show that wybutine side chain may prefer more than one isoenergetic conformation. The intramolecular interactions observed in Fig. 1b–d could be useful to provide structural stability to wybutine side chain at 37th position in presence of codons.

The automated full geometry optimization over the PM3 preferred conformation (Fig. 1b) performed by using RM1, HF-SCF and DFT methods. The RM1 optimized values (Table 3) show resemblance with the PM3 predicted most stable structure (Fig. 1b). Torsion angles α, β, γ, δ, $\psi 1$, $\psi 2$, $\varphi 1$, $\varphi 2$ and ω differ by 15° whereas torsion angle θ deviates by 25° from PM3 preferred values (Fig. 1b). Optimized structure retains hydrogen bonding between O(6)···HC(15), O(6)···HC(16) and O(6)···HN(18) whereas hydrogen bonding between O(20)···HC(17) is not observed in the optimized geometries. The interaction between O(6)···HN(18) is an additional stabilizing factor found in RM1 method which was not observed in PM3 most stable structure (Fig. 1b).

Relative stability of PM3 preferred conformation has also been checked by using computationally expensive quantum chemical *ab-initio* HF-SCF method by using 6-31G** basis set. The optimized torsion angle values are given in Table 3 which show close agreement with PM3 most stable structure (Fig. 1b). The results of complete geometry optimization (Table 3) by using DFT (B3LYP/6-31G**) show that the torsion angles α, β and δ vary by 15° while other torsion angles remain same as compared to PM3 most stable structure (Fig. 1b). The DFT optimized conformation retains similar hydrogen bonding interactions as found in most stable structure (Fig. 1b), additional interaction between O(6) and HN(18) may also provide extra stability to the this optimized structure.

4.2. Conformational preferences of wybutine (yW) by PCILO method

Fig. 2a depicts the predicted most stable conformation of hypermodified nucleic acid base wybutine performed by using

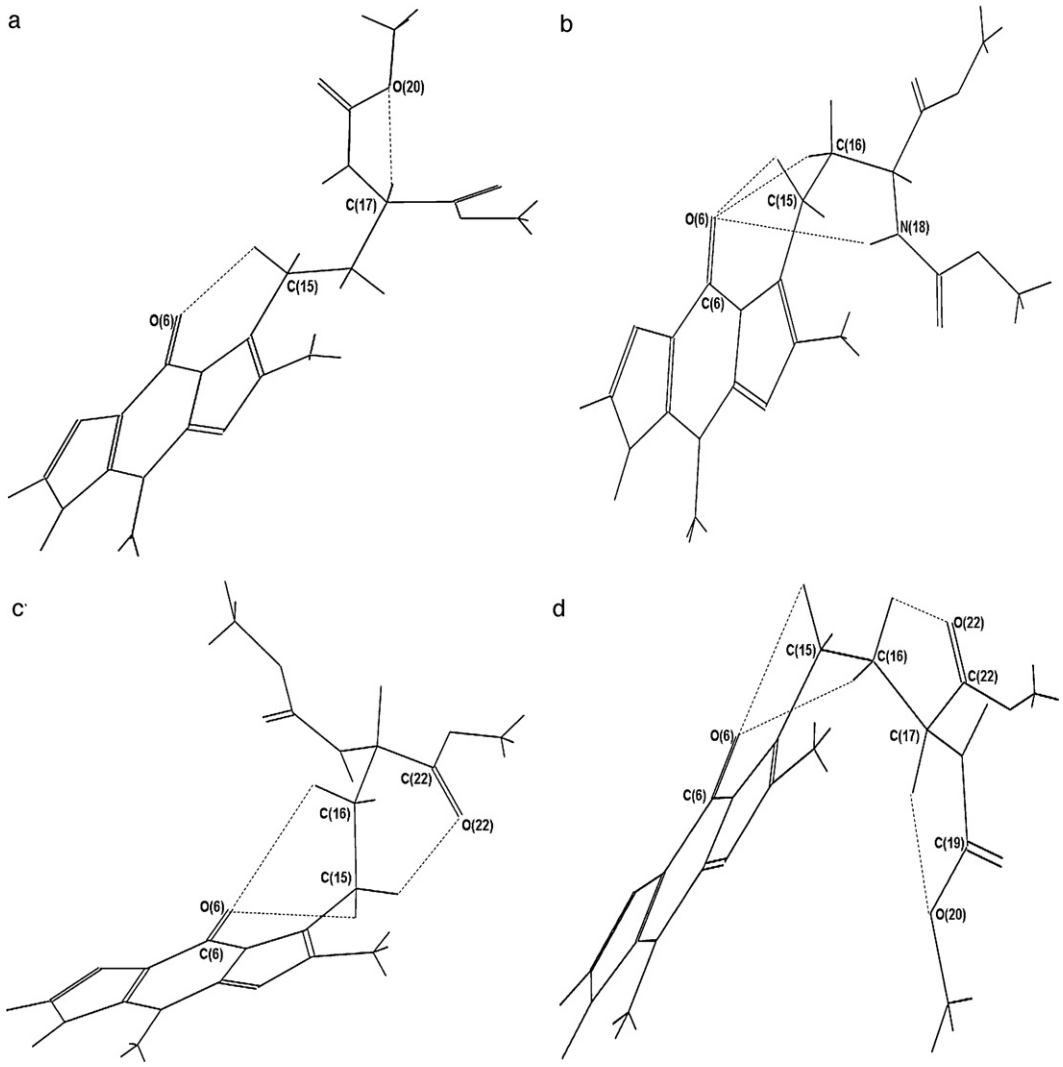

Fig. 3. Molecular dynamics simulation result for 2 ns of wybutine by using PM3 preferred structure as starting geometry: (a) Average structure for 0–300 ps. (b) Average structure for 410–550 ps. (c) Average structure for 1000–1400 ps. (d) Average structure for 1870–1970 ps.

Quantum Chemical Perturbative Configuration Interaction with Localized Orbital (PCILO) method. The torsion angles for the predicted most stable conformation of wybutine are ($\alpha = 120^\circ$, $\beta = 150^\circ$, $\gamma = 300^\circ$, $\delta = 120^\circ$, $\psi 1 = 180^\circ$, $\psi 2 = 180^\circ$, $\theta = 150^\circ$, $\varphi 1 = 180^\circ$, $\varphi 2 = 180^\circ$, $\omega = 180^\circ$). This conformation is stabilized by intramolecular interactions (Table 1) between O(6)···HC(16), O(6)···HN(18) and O(22)···HC(15). The carbonyl oxygen O(6) from modified tricyclic base forms hydrogen bond with the HN(18) and HC(16) of wybutine side chain. Additional stabilization is also expected by interacting O(22) with HC(15). The carboxyl methyl (COOCH3) group of wybutine side chain prefers orientation towards the –CH3 group of five membered tricyclic ring. This kind of orientation is possible may be because of rotation of torsion angles $\gamma = 300^\circ$ and $\delta = 120^\circ$ which results in hydrogen bonding between O(22)···HC(15). Hence, the carboxymethyl (–COOCH3) group of wybutine side chain may also have interactions with codons if present at 3′-end as found in PM3 most stable structure and as suggested by earlier theoretical studies [31,32].

Higher energy (0.13 kcal/mol) alternative stable conformation (Fig. 2b) arises by flipping of torsion angle δ to 300° as compared to PCILO preferred structure (Fig. 2a). This alternative structure is stabilized by hydrogen bonding interactions (Table 1) between O(6)···HC(16), O(6)···HN(18) and O(23)···HC(15). One of the interesting feature in this alternative conformation (Fig. 2b) is that O(23) interacts with HC(15) instead of O(22) as compared to PCILO most stable structure (Fig. 2a) which would be important feature during codon–anticodon interactions according to previous studies [31,32] and PM3 most stable structure (Fig. 1b). Another higher energy (0.25 kcal/mol) alternative conformation arrived by flipping of torsion angle $\varphi 1$ to 0° (Fig. 2c). This conformation may be compared with PM3 most stable structure (Fig. 1b). The hydrogen bonding pattern is found similar as in PCILO most stable structure (Fig. 2a). Flipping of torsion angle α to 240°, γ to 180° and δ to 300° results in another higher energy (2.6 kcal/mole) alternative stable structure (Fig. 2d). Intramolecular interactions between O(6)···HC(16), O(22)···HC(15), and O(23)···HC(16) provide stability to this structure as observed in PCILO preferred structures (Fig. 2a) except O(6)···HN(18).

The alternative stable conformations (Fig. 2b–d) do not differ energetically to large extent as compared to the predicated most stable conformation by PCILO method (Fig. 2a). The torsion angle α may prefer $\pm 120^\circ$ value according to most stable structure (Fig. 2a) and alternative stable structures (Fig. 2b–d) for wybutine side chain. As suggested by earlier experimental studies that anticodon loop is having large conformational changes near the 37th wybutine base in $tRNA^{Phe}$ [26–29], the conformations (Fig. 2b–d) could also change freely during codon–anticodon interactions because their relative energy differences are very less as compared to the

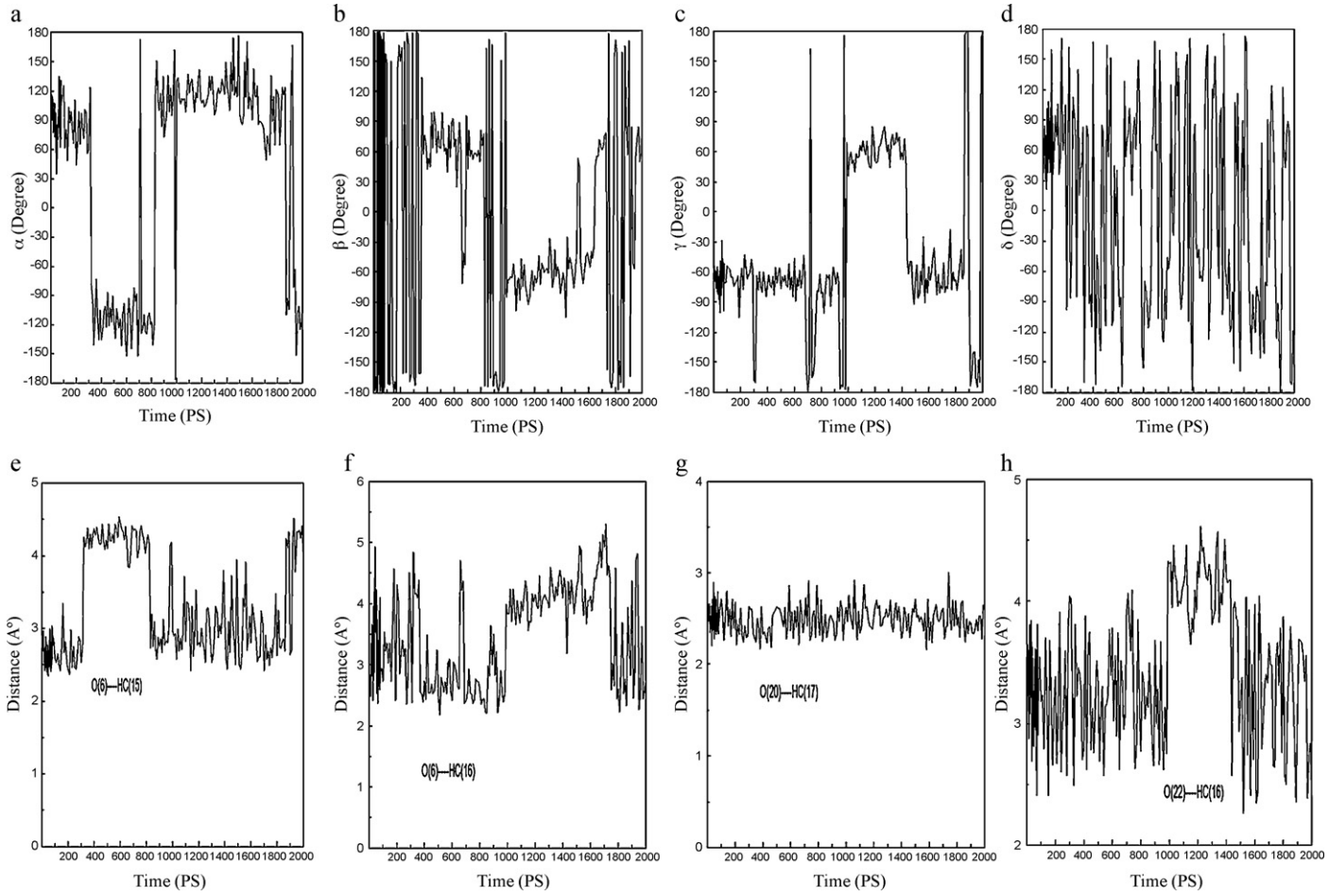

Fig. 4. Molecular dynamics (MD) result: (a) Showing fluctuations in α torsion angle. (b) Fluctuations in β torsion angle. (c) Fluctuations in γ torsion angle. (d) Stabilizing values for δ torsion angle. (e) Fluctuation in hydrogen bonding between O(6)···HC(15), (f) O(6)···HC(16), (g) O(20)···HC(17), (h) O(22)···HC(16).

most stable structure (Fig. 2a). Thus, the PCILO most stable structure (Fig. 2a) and alternative stable structures (Fig. 2b–d) show that wybutine side chain may prefer more than one iso-energetic conformation. The intramolecular interactions observed in Fig. 2a–c could be useful to provide structural stability to wybutine side chain at 37th position in presence of codons.

Automated complete geometry optimization has also been made over the PCILO preferred conformation and alternative stable conformation by quantum chemical semi-empirical methods such as RM1 along with *ab-initio* Hartree–Fock (HF-SCF) and Density Functional Theory (DFT) methods. The results of full geometry optimization by RM1 method over the PCILO preferred structure (Fig. 2a) are given in Table 3. The torsion angles α, β and γ show small differences within the range of 0–23°, while δ and θ torsion angles differ by 48° and 32° respectively. Other torsion angles have negligible difference as compared to PCILO preferred structure (Fig. 2a). Automated geometry optimization by (HF-SCF) using 6-31G** basis set (Table 3) was also carried out over the PCILO preferred structure. The result retains nearly same geometry as like PCILO preferred conformation (Fig. 2a). Full geometry optimization was also performed over PCILO most stable structure (Fig. 2a) by using DFT (B3LYP/6-31G** basis set) method. The optimized values are depicted in Table 3. The torsion angles α, β and θ changes by 10–33° from most stable structure (Fig. 2a), other torsion angles adopts preferred values (Fig. 2a). This optimized conformation maintains similar interactions as found in most stable structure obtained by PM3 (Fig. 1b) and PCILO (Fig. 2a) methods. The hydrogen bonding O(6)···HN(18) is also expected in DFT optimization which is also found as in RM1 and DFT optimization over PM3 most stable structure (Fig. 1b).

4.3. Comparison between PM3 and PCILO conformations

The most stable conformation of wybutine (yW) by PM3 method (Fig. 1b) shows quite similar torsion angle values with PCILO preferred conformation (Fig. 2a), except some minor 30° differences in the α, β and δ torsion angles. This slight change in torsion angles in PCILO preferred structure (Fig. 2a) allows O(6) of tricyclic guanine base to interact with HN(18) and HC(16) of wybutine side chain which is absent in the PM3 preferred structure (Fig. 1b). The torsion angle $\varphi 1$ prefers 0° value in PM3 preferred structure (Fig. 1b) as compared to ($\varphi 1 = 180°$) in case of PCILO preferred structure (Fig. 2a). Due to because of this a weak interaction (Table 1) between O(20)···HC(17) is not possible in case of PCILO preferred conformation as compared to PM3 preferred structure. In the preferred PCILO most stable conformation (Fig. 2a) O(22) interacts with HC(15) instead of HC(16) as observed in the PM3 preferred structure (Fig. 1b). Similarly, O(6) is involved in hydrogen bonding with HC(16) of PCILO most stable structure (Fig. 2a) and HC(15) of PM3 most stable structure (Fig. 1b). Thus, 30° differences in α, β and δ torsion angles also provide different stabilizing factors for the wybutine (yW) side chain.

While comparing the two most stable conformations obtained by PM3 (Fig. 1b) and PCILO (Fig. 2a) methods we found that

both the conformations show 'distal' orientation of wybutine side chain. The hydrogen bonding interactions (Table 1) are different in both the conformations. The PM3 and PCILO most stable conformations maintain the orientation of carboxyl methyl group (COOCH3) of wybutine side chain towards the –CH3 indicated C(13) in the nomenclature (Fig. 1a) group of tricyclic ring. These intramolecular interactions observed by PM3 and PCILO methods are in agreement with crystal structures and shown in the form of supplementary data. Hence, based on the geometrical parameters (Table 1) and torsion angle values (Table 2), we predict that the most stable conformations obtained by PM3 (Fig. 1b) and PCILO method (Fig. 2a) could be the one conformation as shown in earlier experimental studies [26–29]. The relative energy difference found in the most stable and alternative most stable structures obtained by PM3 and PCILO methods are minor. Torsion angle α may prefer $\pm 90^{\circ}$ according to PM3 most stable (Fig. 1b) and alternative stable structures (Fig. 1c and d). Similarly, PCILO most stable structure (Fig. 2a) and alternative stable structures (Fig. 2b–d) the torsion angle α prefers $\pm 120^{\circ}$ value. Based on these conformational results we would like to say that wybutine side chain may prefer exactly two different conformations (conformation I and II) as listed in Table 5 with intramolecular interactions and reference figures.

4.4. Comparison with the crystal structures containing yW at 37th position

Conformational energy calculations of wybutine carried out by PM3 and PCILO methods preserve remarkable features observed in the crystal structure of yW [35,36]. To compare the most stable structures obtained by PM3 and PCILO methods we have separated only wybutine side chain (37th position) from 17 crystal structures and 3 electron microscopy structures containing hypermodified nucleoside wybutine at 3′-adjacent (37th) position in the anticodon loop of yeast $tRNA^{Phe}$ (Table S1, Supplementary data). These structures were taken from Modomics tRNA modification database [56] and protein data bank (www.rcsb.org). These structures differ with each other in its resolution power and its structural properties. Analysis was done for geometrical parameters such as torsion angles and hydrogen bonding interactions of wybutine (yW) base from all crystal structures. On the basis of these criteria, crystal structures have been analyzed and results are mentioned in Table S1, supplementary data. Out of these crystal structures (1EHZ.pdb) [35] show maximum similarity with the most stable structures obtained by PM3 and PCILO methods. The torsion angles and intramolecular hydrogen bonding interactions of wybutine side chain in 1EHZ [35] crystal structure (Fig. 2e) are measured and depicted in Tables 1 and 2. These results strongly support the most stable structures obtained by PM3 and PCILO methods (Figs. 1b and 2a) respectively. Compared with crystal conformer, PM3 preferred conformation retains quite similar torsion angle values for α, γ and $\varphi 1$ where as β and θ torsion angles (Table 2) show small (30°) differences. With reference to crystal structure [35], PCILO preferred structure (Fig. 2a) show common features related with torsion angles and hydrogen bonding interactions with small differences. Hydrogen bonding between O(6)···HN(18) observed in 1EHZ crystal structure [35] is an interesting feature of PCILO preferred structure (Fig. 2a) and RM1, HF-SCF and DFT optimization results over PM3 preferred structure. The geometry optimization of crystal conformer of wybutine base (Fig. 2e) separated from crystal structure (1EHZ.pdb) [35] by using RM1 (Fig. 2f) along with *ab-initio* Hartree–Fock (HF-SCF) and Density Functional Theory (DFT) methods have also been made and results are depicted in Table 3. These optimized results also show resemblance with the most stable structures obtained by PM3 (Fig. 1b) and PCILO (Fig. 2a) methods.

4.5. Molecular dynamics (MD) simulation study

The molecular dynamics (MD) simulations have also been performed to investigate the iso-energetic conformational behavior of wybutine side chain by using Sybyl 7.3 software, commercially available from Tripos, Inc. [54]. PM3 preferred most stable structure of wybutine (Fig. 1b) has been used as a starting geometry for the 2 ns molecular dynamics simulation study. The results of analysis of simulated structures are depicted in Figs. 3 and 4 and Table 4. In order to compare the conformational behavior of wybutine side chain predicted by PM3 and PCILO methods, we have analyzed four different molecular dynamics simulation average structures (Fig. 3a–d) and their geometrical parameters are shown in Table 4. Consistent with the conformational results of PM3 (Fig. 1b) and PCILO (Fig. 2a) most stable structures, the MD simulation average structures 0–300 ps (Fig. 3a), 410–550 ps (Fig. 3b), 1000–1400 ps (Fig. 3c), and 1870–1970 ps (Fig. 3d) also show the 'distal' orientation of wybutine side chain i.e. away from five membered imidazole moiety of tricyclic ring of guanine base. The hydrogen bonding interactions (Table 4) between O(6)···HC(15), O(6)···HN(18), O(6)···HC(16), O(23)···HC(16), O(22)···HC(16) and O(20)···HC(17) also realized in the 2 ns molecular dynamics simulation period as observed in the conformational study of wybutine side chain by using PM3 and PCILO methods.

The results of torsion angles and intramolecular interactions calculated for the average structure (0–300 ps) of molecular dynamics simulation period are found exactly similar as observed in conformational search by PM3 and PCILO methods (Figs. 1b and 2a and c) and depicted in Fig. 3a and Table 4. Torsion angle results and hydrogen bonding parameters (Table 4) of MD simulation average structure at 410–550 ps (Fig. 3b) show resemblance with PM3 alternative most stable structure (Fig. 1d). The intramolecular interactions (Fig. 3b and Table 4) between O(6)···HC(15), O(6)···HC(16), O(6)···HN(18) and N(11)···HN(18) may provide stability for this average structure. Similarly the molecular dynamics simulation average (1000–1400 ps) structure (Fig. 3c) show similarity in hydrogen bonding interactions O(6)···HC(15), O(6)···HC(16), O(22)···HC(16) and O(22)···HC(15) as found in PM3 most stable structure (Fig. 1b) and PCILO most stable structure (Fig. 2a). The interaction between O(23)···HN(18) may provide additional stability for this average structure which did not observe in any other average structures and even PM3 and PCILO most stable structures. The torsion angles of this average structure (1000–1400 ps) show close resemblance with crystal structures (1I9V.pdb) [57] and (1GIX.pdb) [58]. The torsion angles and intramolecular interactions are shown in Fig. 3c and Table 4. The results of last average structure (1870–1970 ps) that we have analyzed are depicted in Fig. 3d and Table 4. This average structure is also stabilized by intramolecular interactions between O(6)···HC(15), O(6)···HC(16), O(22)···HC(16), O(22)···HC(15) and O(20)···HC(17).

Torsion angle α fluctuates periodically between ($\pm 90^{\circ}$ or $\pm 120^{\circ}$) (Fig. 4 and Table 4) over the 2 ns molecular dynamics simulation period, which is similar as compared to PM3 (Fig. 1b) and PCILO (Fig. 2a) most stable structures. Similarly, this periodic fluctuation of torsion angle α ($\pm 90^{\circ}$ or $\pm 120^{\circ}$) also observed in slightly higher energy alternative stable structures of PM3 (Fig. 1c and d) and PCILO (Fig. 2b–d). The fluctuations of all the torsion angles within the range of (0–300 ps, 410–550 ps, 1000–1400 ps, and 1970–2000 ps) are shown in Table 4 and found similar in comparison with PM3 and PCILO preferred structures (Table 2). The hydrogen bonding between O(6)···HC(15) observed in PM3 most stable and alternative stable structures (Fig. 1b–d) is also maintained during MD simulation time period (0–300 ps) when torsion angle α prefers 90° value. As soon as torsion angle α shifts to 240° for the simulation period (301–800 ps), the interaction between O(6)···HC(15) (Fig. 4e) breaks up and instead the structure is stabilized by

Table 4
Geometrical parameters for torsion angles and hydrogen bonding interactions for average structure and snapshot structures after MD simulation study of PM3 most stable structure (Fig. 1b).

Average structures/snapshots (ps)	Torsion angle (degree)	Atoms involved (1–2–3)	Distance atom pair 1–2 (A°)	Angle 1–2–3 (degree)	Figure Ref.
0–300	$\alpha = 85^\circ$, $\beta = 179^\circ$, $\gamma = 295^\circ$, $\delta = 57^\circ$, $\psi 1 = 181^\circ$, $\psi 2 = 146^\circ$, $\theta = 159^\circ$, $\varphi 1 = 356^\circ$, $\varphi 2 = 179^\circ$, $\omega = 180^\circ$	O(6)···HC(15) O(6)···HC(16) O(20)···HC(17)	2.233 2.505 1.792	100.5 117.4 108.9	3a
880	$\alpha = 83^\circ$, $\beta = 166^\circ$, $\gamma = 287^\circ$, $\delta = 83^\circ$, $\psi 1 = 156^\circ$, $\psi 2 = 197^\circ$, $\theta = 165^\circ$, $\varphi 1 = 14^\circ$, $\varphi 2 = 142^\circ$, $\omega = 174^\circ$	O(6)···HC(15) O(22)···HC(16) O(23)···HC(16)	2.573 2.842 2.799	116.73 94.63 97.39	–
830–930	$\alpha = 122^\circ$, $\beta = 182^\circ$, $\gamma = 281^\circ$, $\delta = 199^\circ$, $\psi 1 = 202^\circ$, $\psi 2 = 227^\circ$, $\theta = 120^\circ$, $\varphi 1 = 357^\circ$, $\varphi 2 = 168^\circ$, $\omega = 168^\circ$	O(6)···HC(15) O(6)···HC(16) O(20)···HC(17)	2.416 2.141 1.710	101.37 116.73 92.24	–
1760–1840	$\alpha = 102^\circ$, $\beta = 182^\circ$, $\gamma = 297^\circ$, $\delta = 51^\circ$, $\psi 1 = 183^\circ$, $\psi 2 = 206^\circ$, $\theta = 152^\circ$, $\varphi 1 = 356^\circ$,$\varphi 2 = 172^\circ$, $\omega = 137^\circ$	O(6)···HC(15) O(6)···HC(16) O(20)···HC(17)	2.607 2.699 2.213	100.00 114.46 94.52	–
410–550	$\alpha = 248^\circ$, $\beta = 86^\circ$, $\gamma = 284^\circ$, $\delta = 229^\circ$, $\psi 1 = 181^\circ$, $\psi 2 = 181^\circ$, $\theta = 159^\circ$, $\varphi 1 = 1^\circ$, $\varphi 2 = 187^\circ$, $\omega = 208^\circ$	O(6)···HC(15) O(6)···HC(16) O(6)···HN(18) N(11)···HN(18)	2.345 2.037 2.417 2.248	101.37 137.41 133.11 105.16	3b
750	$\alpha = 234^\circ$, $\beta = 58^\circ$, $\gamma = 210^\circ$, $\delta = 104^\circ$, $\psi 1 = 189^\circ$, $\psi 2 = 188^\circ$, $\theta = 75^\circ$, $\varphi 1 = 23^\circ$, $\varphi 2 = 186^\circ$, $\omega = 154^\circ$	O(6)···HC(16) O(20)···HC(17) O(22)···HC(15)	2.373 2.316 2.742	101.37 137.41 109.48	–
730–770	$\alpha = 238^\circ$, $\beta = 56^\circ$, $\gamma = 224^\circ$, $\delta = 109^\circ$, $\psi 1 = 175^\circ$, $\psi 2 = 121^\circ$, $\theta = 141^\circ$, $\varphi 1 = 7^\circ$, $\varphi 2 = 184^\circ$, $\omega = 154^\circ$	O(6)···HC(15) O(6)···HC(16) O(20)···HC(17) O(22)···HC(15)	2.497 2.231 1.952 2.910	99.36 127.03 105.34 98.35	–
1870–1970	$\alpha = 249^\circ$, $\beta = 71^\circ$, $\gamma = 199^\circ$, $\delta = 154^\circ$, $\psi 1 = 158^\circ$, $\psi 2 = 173^\circ$, $\theta = 116^\circ$, $\varphi 1 = 353^\circ$, $\varphi 2 = 148^\circ$, $\omega = 190^\circ$	O(6)···HC(15) O(6)···HC(16) O(20)···HC(17) O(22)···HC(16) O(22)···HC(15)	2.430 2.385 1.385 1.912 2.110	131.69 150.23 110.61 105.70 140.23	3d
1000–1400	$\alpha = 109^\circ$, $\beta = 278^\circ$, $\gamma = 69^\circ$, $\delta = 178^\circ$, $\psi 1 = 164^\circ$, $\psi 2 = 133^\circ$, $\theta = 78^\circ$, $\varphi 1 = 359^\circ$, $\varphi 2 = 176^\circ$, $\omega = 195^\circ$	O(6)···HC(15) O(6)···HC(16) O(22)···HC(16) O(22)···HC(15) O(23)···HN(18)	1.793 1.852 1.671 1.706 1.953	110.13 134.40 97.67 128.20 101.76	3c

O(6)···HC(16) (Fig. 4f) similarly as found in PCILO most stable structure and alternative stable structures (Fig. 2a–d). Then for the further simulation period (801–1920 ps) the interaction between O(6)···HC(15) is retained similar to structures found in PM3 conformational search (Fig. 1b–d). The other intramolecular interactions between O(6)···HN(18), O(20)···HC(17), O(22)···HC(16) and O(23)···HC(16) are also maintained during the 2 ns MD simulation period (Fig. 4 and Table 4) as observed in PM3 and PCILO conformational study.

Based on the earlier literature [26–29] wybutine has more than two conformations in aqueous solvent system. Our PM3 and PCILO conformational search results along with MD simulation results show that wybutine may prefer three different conformations. The torsion angles and geometrical parameters of the three different conformations are shown in Table 5.

4.6. Concept of multiple iso-energetic conformations for wybutine side chain

During salvation effect, wybutine (yW) side chain show three different but unique conformations (Table 5) having different torsion angle values but almost similar intramolecular interactions at specific intervals of time period over the 2 ns of molecular dynamics simulation period (Figs. 3a–d and 4a–h). As mentioned earlier in literature, wybutine shows two [26] or three [29] different conformations in aqueous solvent, our conformational study (Figs. 1b–d and 2a–d) and molecular dynamics (MD) simulation data also supports multiple conformations for the wybutine (yW) side chain (Table 5).

Predicted most stable structure of wybutine (Fig. 1b) by PM3 conformational analysis preserves torsion angle values and intramolecular hydrogen bonding interactions from crystal structure conformer (1EHZ) of wybutine. Even though automated complete geometry optimization by RM1, HF-SCF and DFT calculations over the PM3 and PCILO predicted preferred conformations retain all salient features observed in crystal structure conformer (1EHZ) and its optimization results. The first higher energy (0.36 kcal/mol) (Fig. 1c) alternative stable structure of wybutine differ only in α torsion angle which deviate by 180° from its predicted value 90° and positioned to 270°. Similarly, in the second higher energy (0.4 kcal/mol) alternative stable conformation (Fig. 1d) α and δ torsion angles also change by 180° as compared to preferred structure (Fig. 1b). Even this change in α and δ torsion angles, alternative structures (Fig. 1c and 1d) preserve all hydrogen bonding interactions from PM3 preferred (Fig. 1b) as well as crystal structure conformer (1EHZ) [35]. These results show that the wybutine (yW) may be found in two different unique conformations having some change in dihedral angle but show similar hydrogen bonding interactions. Also PCILO predicted structure and its higher energy alternative structures show close agreement with PM3 calculation results and supports the multiple conformation nature of wybutine (yW) side chain.

The molecular dynamics (MD) simulation result show that most stable structure (conformation I) obtained by PM3 method (Fig. 1b) as a starting geometry was maintained for the period (0–300 ps, Fig. 3a) (830–930 ps), snapshot 880 ps (1760–1840 ps), and thereafter wybutine side chain prefers another conformation (conformation II) from (410–550 ps, Fig. 3b) (730–770 ps), snapshot 750 ps (1870–1970 ps) where wybutine has different torsion angle values but same intramolecular interactions as found in the alternative stable structures obtained by PM3 (Fig. 1c and d) and PCILO (Fig. 2b–d) methods.

Table 5
Torsion angles and hydrogen bonding interactions of three different iso-energetic conformers of wybutine side chain obtained by PM3, PCILO and MD simulation methods.

Conformation No.:	Torsion angles (degree)	Atoms Involved (1–2–3)	Distance atom pair 1–2 (A°)	Angle 1–2–3 (degree)	(PM3/PCILO/MD) Figure Ref.
Conformation I	$\alpha = 90^\circ$, $\beta = 180^\circ$, $\gamma = 300^\circ$, $\delta = 90^\circ$, $\psi 1 = 180^\circ$, $\psi 2 = 180^\circ$, $\theta = 150^\circ$, $\varphi 1 = 0^\circ$, $\varphi 2 = 180^\circ$, $\omega = 180^\circ$	O(6)···HC(15)	2.428	110.93	1b, 3a
		O(20)···HC(17)	2.581	94.61	
		O(22)···HC(16)	2.713	98.32	
		O(23)···HC(16)	2.750	98.77	
	$\alpha = 120^\circ$, $\beta = 150^\circ$, $\gamma = 300^\circ$, $\delta = 120^\circ$, $\psi 1 = 180^\circ$, $\psi 2 = 180^\circ$, $\theta = 150^\circ$, $\varphi 1 = 0^\circ$, $\varphi 2 = 180^\circ$, $\omega = 180^\circ$	O(6)···HC(16)	2.181	117.24	2c, 3a
		O(6)···HN(18)	1.767	157.11	
		O(22)···HC(15)	2.452	93.52	
	$\alpha = 120^\circ$, $\beta = 150^\circ$, $\gamma = 300^\circ$, $\delta = 120^\circ$, $\psi 1 = 180^\circ$, $\psi 2 = 180^\circ$, $\theta = 150^\circ$, $\varphi 1 = 180^\circ$, $\varphi 2 = 180^\circ$ $\omega = 180^\circ$	O(6)···HC(16)	2.181	117.24	2a, 3a
		O(6)···HN(18)	1.767	157.11	
		O(22)···HC(15)	2.452	93.52	
Conformation II	$\alpha = 270^\circ$, $\beta = 180^\circ$, $\gamma = 300^\circ$, $\delta = 270^\circ$, $\psi 1 = 180^\circ$, $\psi 2 = 180^\circ$, $\theta = 150^\circ$, $\varphi 1 = 0^\circ$, $\varphi 2 = 180^\circ$, $\omega = 180^\circ$	O(6)···HC(15)	2.428	110.93	1d, 3b,3d
		O(20)···HC(17)	2.581	94.61	
		O(22)···HC(16)	2.709	98.51	
		O(23)···HC(16)	2.753	98.57	
	$\alpha = 240^\circ$, $\beta = 150^\circ$, $\gamma = 180^\circ$, $\delta = 300^\circ$, $\psi 1 = 180^\circ$, $\psi 2 = 180^\circ$, $\theta = 150^\circ$, $\varphi 1 = 180^\circ$, $\varphi 2 = 180^\circ$, $\omega = 180^\circ$	O(6)···HC(16)	2.169	118.05	2d, 3b,3d
		O(22)···HC(15)	2.661	131.09	
		O(23)···HC(16)	2.702	93.81	
	$\alpha = 270^\circ$, $\beta = 180^\circ$, $\gamma = 300^\circ$, $\delta = 90^\circ$, $\psi 1 = 180^\circ$, $\psi 2 = 180^\circ$, $\theta = 150^\circ$, $\varphi 1 = 0^\circ$, $\varphi 2 = 180^\circ$, $\omega = 180^\circ$	O(6)···HC(15)	2.428	110.93	1c, 3b,3d
		O(20)···HC(17)	2.581	94.61	
		O(22)···HC(16)	2.713	98.32	
		O(23)···HC(16)	2.750	98.77	
Conformation III	MD average structure (1000–1400 ps) $\alpha = 109^\circ$, $\beta = 278^\circ$, $\gamma = 69^\circ$, $\delta = 178^\circ$, $\psi 1 = 164^\circ$, $\psi 2 = 133^\circ$, $\theta = 78^\circ$, $\varphi 1 = 359^\circ$, $\varphi 2 = 176^\circ$, $\omega = 195^\circ$	O(6)···HC(15)	1.793	110.13	3c, 1I9V.pdb [57] 1GIX.pdb [58]
		O(6)···HC(16)	1.852	134.40	
		O(22)···HC(16)	1.671	97.67	
		O(22)···HC(15)	1.706	128.20	
		O(23)···HN(18)	1.953	101.76	

MD simulation average structure for the period (1000–1400 ps) depicted in Fig. 3c show different geometry as compared to other two conformations (conformation I and II) as discussed above. The torsion angles and hydrogen bonding parameters are listed in Table 4. The intramolecular interactions are stronger as obtained in other two conformations (conformation I and II). In this conformation the torsion angles $\beta = 278^\circ$, $\gamma = 69^\circ$, $\delta = 178^\circ$ and $\theta = 78^\circ$ prefers different values which we did not observe in the above discussed MD structures (Fig. 3a, b and d) as well as in the conformational study by PM3 (Fig. 1b–d) and PCILO (Fig. 2a–d) methods. This conformation occurs only for (1000–1400 ps) time period and do not fluctuate regularly as like conformation I and II till rest of the 2 ns molecular dynamics simulation period. Hence, here we predict that this could be the third conformation that wybutine side chain might prefer as discussed in earlier experimental study [29]. This structure of wybutine side chain (conformation III) is also in agreement with some crystal structures [57,58] and shown in the form of Table S1, Supplementary data.

5. Conclusion

Conformational analysis of hypermodified nucleic acid base wybutine (yW) by quantum chemical semi-empirical PM3 and PCILO methods along with molecular dynamics (MD) simulation shows that wybutine side chain may prefer three different conformations as shown in Table 5. All these conformations (conformation I, II, and III) are in close agreement with available crystal structures of $tRNA^{Phe}$ containing hypermodified nucleic acid base wybutine in the anticodon loop. The interaction between O(6) of modified tricyclic base with C(15) and C(16) of wybutine side chain may help maintain 'distal' conformation. The intramolecular interactions between carboxyl oxygen O(22)···HC(16), O(23)···HC(15) allow us to predict that the atoms O(22) and O(23) could be accessible to participate in recognition with codons if present at the 3′-side of the anticodon loop. These two interactions are also maintained during the simulation period in all the three different conformations of wybutine. Conformational analysis data as well as MD

simulation data show similar results as found in crystal structures (Table S1, Supplementary data). Thus, wybutine side chain may prefer multiple iso-energetic conformations according to our conformational search results obtained by (PM3, PCILO) as well as molecular dynamic (MD) simulations carried on the PM3 preferred structure.

As we know that lack of hypermodified nucleic acid base wybutine in $tRNA^{Phe}$ could cause some pathological consequences such as; $tRNA^{Phe}$ from neuroblastoma cells and ascite tumor cells lacks the fully modified yW base [21]. $tRNA^{Phe}$ that lacks the yW modification has been shown to enhance frameshifting and influence the replication of human immunodeficiency virus [20,21]. Thus, preferred multiple conformations of wybutine at the 3′-adjacent (37th) position to anticodon loop of $tRNA^{Phe}$ may have functional role in preventing incorrect Watson–Crick base pairing during codon–anticodon interactions and thus could play role in frameshift mutations. Hence this structural study of hypermodified nucleic acid base wybutine may be helpful to understand the role of wybutine in pathological consequences of many diseases such as Cancer and HIV.

Acknowledgements

NMK is gratefully acknowledged to Lady Tata Memorial Trust, Mumbai, India, for providing Junior Scholarship. Financial support sanctioned to KDS by Department of Science and Technology (DST), New Delhi is gratefully acknowledged.

Appendix A. Supplementary data

Supplementary data associated with this article can be found, in the online version, at doi:10.1016/j.jmgm.2011.03.005.

References

[1] J.A. McCloskey, S. Nishimura, Modified nucleosides in transfer RNA, Acc. Chem. Res. 10 (1977) 403–410.
[2] G.R. Bjork, J.U. Ericson, C.E.D. Gustafsson, T.G. Hagervall, Y.H. Jonsson, P.M. Wikstrom, Transfer RNA modification, Annu. Rev. Biochem. 56 (1987) 263–287.
[3] M. Sprinzl, C. Horn, M. Brown, A. Ludovitch, S. Steinberg, Compilation of tRNA sequences and sequences of tRNA genes, Nucleic Acids Res. 26 (1998) 148–153.
[4] R.W. Adamiak, P. Gornicki, Hypermodified nucleosides of tRNA: synthesis, chemistry, and structural features of biological interest, Prog, Nucleic Acids Res. Mol. Biol. 32 (1985) 27–74.
[5] Y. Motorin, G. Bec, R. Tewari, H. Grosjean, Transfer RNA recognition by the *Escherichia coli* Δ^2-isopentenyl-pyrophosphate: tRNA Δ^2-isopentenyl transferase: dependence on the anticodon arm structure, RNA 3 (1997) 721–733.
[6] A. Morin, S. Auxilien, B. Senger, R. Tewari, H. Grosjean, Structural requirements for enzymatic formation of threonylcarbamoyladenosine (t6A) in tRNA: an in vivo study with *Xenopus laevis* oocytes, RNA 4 (1998) 24–37.
[7] S. Yokoyama, S. Nishimura, Modified nucleosides and codon recognition, in: D. Soll, U.L. Rajbhandary (Eds.), tRNA Structure, Biosynthesis, and Function, ASM Press, Washington, DC, 1995, pp. 207–223.
[8] M.T. Watts, I. Tinoco, Role of hypermodified bases in transfer RNA. Solution properties of dinucleoside monophosphates, Biochemistry 17 (1978) 2455–2463.
[9] H. Grosjean, S. deHenan, D.M. Crothers, on the physical basis for ambiguity in genetic coding interactions, Proc. Natl. Acad. Sci. U.S.A. 75 (1978) 610–614.
[10] S. Nishimura, Minor components in transfer RNA: their characterization, location, and function, Prog. Nucleic Acid Res. Mol. Biol. 12 (1972) 49–85.
[11] P.F. Agris, The importance of being modified: roles of modified nucleosides and Mg^{2+} in RNA structure and function, Prog. Nucleic Acid Res. Mol. Biol. 53 (1996) 79–129.
[12] G.R. Bjork, Modified nucleosides at position 34 and 37 of tRNAs and their predicted coding capacities, in: H. Grosjean, R. Benne (Eds.), Modification and Editing of RNA, ASM Press, Washington, DC, 1998, pp. 579–583.
[13] M. Yarus, Translational efficiency of transfer RNAs: uses of an extended anticodon, Science 218 (1982) 646–652.
[14] T.H. Tsang, B.N. Ames, M. Buck, Sequence specificity of tRNA-modifying enzymes an analysis of 258 tRNA sequences, Biochim. Biophys. Acta 741 (1983) 180–196.
[15] U.L. RajBhandary, S.H. Chang, A. Stuart, R.D. Faulkner, R.M. Hoskinson, H.G. Khorana, Studies on polynucleotides. LXVIII. The primary structure of yeast phenylalanine transfer RNA, Proc. Nat. Acad. Sci. U.S.A. 57 (1967) 751–758.
[16] K. Nakanishi, F.F. urutachi, M. Funamizu, D. Grunberger, I. Weinstein, Structure of the fluorescent Y base from yeast phenylalanine transfer ribonucleic Acid, J. Am. Chem. Soc. 92 (1970) 7617–7619.
[17] B.S. Dudock, G. Katz, E.K. Taylor, R.W. Holley, Primary structure of wheat germ phenylalanine transfer RNA, Proc. Natl. Acad. Sci. U.S.A. 62 (1969) 941–945.
[18] H. Kasai, M. Goto, K. Ikeda, M. Zama, Structure of Wye (Yt Base) and Wyosine (Yt) from *Torulopsis utilis* phenylalanine transfer ribonucleic acid, Biochemistry 15 (1976) 898–904.
[19] A. Noma, T. Suzuki, Ribonucleome analysis identified enzyme genes responsible for wybutosine synthesis, Nucleic Acids Sympos. Ser. 50 (2006) 65–66.
[20] B.A. Carlson, S.Y. Kwon, M. Chamorro, S. Oroszlan, D.L. Hatfield, B.J. Lee, Transfer RNA modification status influences retroviral ribosomal frameshifting, Virology 255 (1999) 2–8.
[21] D. Hatfield, Y.X. Feng, B.J. Lee, A. Rein, J.G. Levin, S. Oroszlan, Chromatographic analysis of the aminoacyl-tRNAs which are required for translation of codons at and around the ribosomal frameshift sites of HIV, HTLV-1, and BLV, Virology 173 (1989) 736–742.
[22] W.F. Waas, Z. Druzina, M. Hanan, P. Schimmel, Role of a tRNA base modification and its precursors in frameshifting in eukaryotes, J. Biol. Chem. 282 (2007) 26026–26034.
[23] Y. Kuchino, E. Borek, D. Grunberger, J. Mushinski, S. Nishimura, Changes of post-transcriptional modification of wye base in tumor-specific $tRNA^{Phe}$, Nucleic Acids Res. 10 (1982) 6421–6432.
[24] W.J. Krzyzosiak, J. Ciesiolka, Long-range conformational transition in yeast $tRNA^{Phe}$, induced by the Y-base removal and detected by chloroacetaldehyde modification, Nucleic Acids Res. 11 (1983) 6913–6921.
[25] D.R. Kearns, K.L. Wong, Y.P. Wong, Effect of the removal of the Y base on the conformation of yeast $tRNA^{Phe}$, Proc. Nat. Acad. Sci. U.S.A. 70 (1973) 3843–3846.
[26] D. Labuda, D. Porschke, Magnesium ion inner sphere complex in the anticodon loop of phenylalanine transfer ribonucleic acid, Biochemistry 21 (1982) 49–53.
[27] R. Ehrlich, J.F. Lefevre, P. Remy, Fluorimetric study of the complex between yeast phenylalanyl-tRNA synthetase and $tRNA^{Phe}$, Eur. J. Biochem. 103 (1980) 145–153.
[28] C. Urbanke, G. Mass, A novel conformational change of the anticodon region of $tRNA^{Phe}$ (yeast), Nucleic Acids Res. 5 (1978) 1551–1560.
[29] F. Claesens, R. Rigler, Conformational dynamics of the anticodon loop in yeast $tRNA^{Phe}$ as sensed by the fluorescence of wybutine, Eur. Biophys. J. 13 (1986) 331–342.
[30] A. Lahiri, J. Ulicny, A. Laaksonen, Theoretical analysis of the excited state properties of wybutine: a natural probe for transfer RNA dynamics, Int. J. Mol. Sci. 5 (2004) 76–84.
[31] M.D. Neto, M.S. Giambiagi, M. Giambiagi, Influence of the hypermodified Y base on the A.U pairing in codon–anticodon interaction, Chem. Phys. Lett. 290 (1998) 205–210.
[32] A.S. Werneck, M.D. Neto, E.R. Maia, The hypermodified Y base electrostatic contribution to the energetics of the codon–anticodon pairing in $tRNA^{Phe}$, J. Mol. Struct. (Theochem) 427 (1998) 15–23.
[33] A. Lahiri, L. Nilsson, Molecular dynamics of the anticodon domain of yeast $tRNA^{Phe}$: codon–anticodon interaction, Biophys. J. 79 (2000) 2276–2289.
[34] O. Kennard, in: R.C. Weast, M.J. Astle (Eds.), CRC Handbook of Chemistry and Physics, CRC Press, Boca Raton, 1980–1981, pp. 208–211.
[35] H. Shi, P.B. Moore, The crystal structure of yeast phenylalanine tRNA at 1.93 Å resolution: a classic structure revisited, RNA 6 (2000) 1091–1105.
[36] S.R. Holbrook, J.L. Sussman, R.W. Warrant, S.H. Kim, Crystal structure of yeast phenylalanine transfer RNA. II. Structural features and functional implications, J. Mol. Biol. 123 (1978) 631–660.
[37] S. Diner, J.P. Malrieu, P. Claverie, Localized bond orbitals and the correlation problem, Theor. Chim. Acta 13 (1969) 1–17.
[38] S. Diner, J.P. Malrieu, F. Jordan, M. Gilbert, Localized bond orbitals and the correlation problem. III. Energy to third order in the zero differential overlap approximation. Application to sigma electron systems, Theor. Chim. Acta 15 (1969) 100–110.
[39] A. Masson, B. Levy, J.P. Malrieu, Formaldehyde calculation of energy in the ground state by a perturbation methods, Theor. Chim. Acta 18 (1970) 193–207.
[40] B. Pullman, A. Pullman, Molecular orbital calculations on the conformation of amino acid residues of proteins, Adv. Protein Chem. 16 (1974) 347–526.
[41] B. Pullman, A. Saran, Quantum-mechanical studies on the conformation of nucleic acids and their constituents, Prog. Nucleic Acid Res. Mol. Biol. 18 (1976) 216–326.
[42] R. Tewari, Theoretical studies on conformational preferences of modified nucleic acid base N^6-(N-glycylcarbonyl) adenine, Int. J. Quant. Chem. 31 (1987) 611–624.
[43] R. Tewari, Conformational preferences of modified nucleic acid bases N^6-methyl-N^6-(N-threonylcarbonyl) adenine and 2-methylthion-N^6-(N-threonylcarbonyl)adenine by quantum chemical PCILO Calculations, J. Biomol. Struct. Dyn. 8 (1990) 675–686.
[44] R. Tewari, N(7)-protonation-induced conformational flipping in hypermodified nucleic acid base N6-(N-glycylcarbonyl) adenine, Chem. Phys. Lett. 238 (1995) 365–370.
[45] U.B. Sonavane, K.D. Sonawane, A. Morin, H. Grosjean, R. Tewari, N(7)-protonation induced conformational flipping in hypermodified nucleic acid bases N6-(N-threonylcarbonyl) adenine and its 2-methylthio- or N(6)-methyl-derivatives, Int. J. Quant. Chem. 75 (1999) 223–229.
[46] K.D. Sonawane, U.B. Sonavane, R. Tewari, Conformational flipping of the N(6) substituent in diprotonated N6-(N-glycylcarbonyl) adenines: the role of N(6)

H in purine ring protonated ureido adenines, Int. J. Quant. Chem. 78 (2000) 398–405.
[47] K.D. Sonawane, R. Tewari, Conformational preferences of hypermodified nucleoside lysidine (k^2C) occurring at 'wobble' position in anticodon loop of $tRNA^{Ile}$, Nucleos. Nucleot. Nucleic Acids 27 (2008) 1158–1174.
[48] U.B. Sonavane, K.D. Sonawane, R. Tewari, Conformational preferences of the base substituent in hypermodified nucleotide Queosine 5′-monophosphate 'pQ' and protonated variant 'QH+', J. Biomol. Struct. Dyn. 20 (2002) 437–485.
[49] K.D. Sonawane, U.B. Sonavane, R. Tewari, Conformational preferences of anticodon 3′-adjacent hypermodified nucleic acid base cis-or trans-Zeatin and its 2-methylthio derivative, cis- or trans-ms^2Zeatin, J. Biomol. Struct. Dyn. 19 (2002) 637–648.
[50] W.J. Hehre, L. Radom, P.V.R. Schleyer, J.A. Pople, Ab Initio Molecular Orbital Theory, Wiley, New York, 1986.
[51] G.B. Rocha, R.O. Reire, A.M. Simas, J.J.P. Stewart, RM1: a reparameterization of AM1 for H, C, N, O, P, S, F, Cl, Br and I, J. Comp. Chem. 27 (2006) 1101–1111.
[52] A.D. Becke, Density-functional thermochemistry. III. The role of exact Exchange, J. Chem. Phys. 98 (1993) 5648–5652.
[53] M.M. Francl, W.J. Pietro, W.J. Hehre, J.S. Binkley, M.S. Gordon, D.J. Defrees, J.A. Pople, Self-consistent molecular orbital methods. XXIII. A polarization-type basis set for second-row elements, J. Chem. Phys. 77 (1982) 3654–3665.
[54] Tripos International, SYBYL 7.3, Tripos International, South Hanley Rd., St. Louis, Missouri, USA, 2006.
[55] C.J. Weiner, P.A. Kollman, D.A. Case, U.C. Singh, C. Ghio, G. Alaqom, S. Protera, P.J. Weiner, A new force field for molecular mechanical simulation of nucleic acids and proteins, J. Am. Chem. Soc. 106 (1984) 765–784.
[56] D.S. Horkawicz, A. Czerwoniec, M.J. Gajda, M. Feder, H. Grosjean, J.M. Bujnicki, MODOMICS: a database of RNA modification pathways, Nucleic Acids Res. 34 (2006) D145–D149 (Database issue).
[57] N.E. Mikkelsen, K. Johansson, A. Virtanen, L.A. Kirsebom, Aminoglycoside binding displaces a divalent metal ion in a tRNA-neomycin B Complex, Nat. Struct. Biol. 8 (2001) 510–514.
[58] M.M. Yusupov, G.Z. Yusupova, A. Baucom, K. Lieberman, T.N. Earnest, J.H.D. Cate, H.F. Noller, Crystal structure of the ribosome at 5.5 Å resolution, Science 292 (2001) 883–896.